# Synthesis and vibrational spectroscopy of halotrichite and bilinite

**Sara J. Palmer, B. Jagannadha Reddy and Ray L. Frost** •

Chemistry Discipline, Faculty of Science, Queensland University of Technology, GPO Box 2434, Brisbane Queensland 4001, Australia.

## Abstract

Near infrared (NIR), infrared (IR) spectroscopy and X-ray diffraction (XRD) have been applied to halotrichites of the formula $FeAl_2(SO_4)_4 \cdot 22H_2O$ and $Fe^{2+}Fe_2^{3+}(SO_4)_4 \cdot 22H_2O$. Comparison of the halotrichites and their starting materials has been used to give a better understanding of the bonding involved in these types of minerals. The vibrational spectroscopy data has shown that $Fe^{2+}$ oxidises during the formation of halotrichite, no preventative measures were implemented to prevent oxidation, and this has been clearly shown by the position and broadness of electronic bands of transition metals in the NIR spectra (12500 to 7500 $cm^{-1}$). It is apparent from this region that $Fe^{3+}$ substitutes for $Al^{3+}$ in the synthesis of halotrichite. Due to the oxidation of $Fe^{2+}$ to $Fe^{3+}$ the halotrichite sample contains a small portion of bilinite. This has been confirmed by XRD, peaks at 9 and 14° 2θ were observed in the halotrichite sample and are identical to the XRD pattern obtained for bilinite. Substitution of aluminium for $Fe^{3+}$ has resulted in significant changes in the overall infrared and NIR spectral profiles. However, the lower wavenumber regions of the NIR spectra have very similar spectral profiles, which indicate a similar structure to halotrichite has formed for bilinite. This work has shown that iron halotrichites can be synthesised and characterised by infrared and NIR spectroscopy.

*Key words***:** halotrichite; bilinite; iron; NIR spectroscopy; infrared spectroscopy.

• Author to whom correspondence should be addressed (r.frost@qut.edu.au)

## Introduction

The halotrichite mineral series are related to alum $R_2SO_4 \cdot M_2(SO_4)_3 \cdot 24H_2O$ or $RM(SO_4)_2 \cdot 12H_2O$ minerals where R represents an atom of a univalent ion such as ammonium, lithium, sodium, potassium and caesium and where M represents a trivalent metal such as aluminium, iron, chromium, and gallium. When a divalent anion is introduced instead of the monovalent atom, such as manganese, ferrous iron, cobalt, zinc and magnesium a double sulphate will form. These double sulphates form the halotrichite mineral series. Halotrichite has the following formula: $FeAl_2(SO_4)_4 \cdot 22H_2O$ or $Fe(SO_4) \cdot Al_2(SO_4)_3 \cdot 22H_2O$. These minerals are all isomorphous and crystallise in the monoclinic space group $P2_{1/c}$. In the structure four crystallographically independent sulphate ions are present [1]. One acts as a unidentate ligand to the $M^{2+}$ ion and the other three are involved in complex hydrogen bond arrays involving coordinated water molecules to both cations and to the lattice water molecules.

Ross reported that halotrichite has infrared bands associated with sulphate at 1000 $cm^{-1}$ ($\nu_1$), 480 $cm^{-1}$ ($\nu_2$) , 1121, 1085 and 1068 $cm^{-1}$ ($\nu_3$), 645 and 600 $cm^{-1}$ ($\nu_4$) [2]. These minerals display infrared water bands in the OH stretching region, 3400 and 3000 $cm^{-1}$ region; OH deformation, 1650 $cm^{-1}$ region, OH liberation, 725 $cm^{-1}$ region [2]. Ross also reports a weak band at ~960 $cm^{-1}$ assigned to a second OH librational mode. In the structure, six water molecules surround each of the two cations. This means the sulphate ions are distant from the cations and coordinate to the water molecules.

In this work we report the infrared and near-infrared spectra of two synthetic halotrichites and compare the spectra with the starting materials from which they were synthesised. The synthetic halotrichites discussed in this investigation are halotrichite ($Fe^{2+}Al_2^{3+}(SO_4)_4 \cdot 22H_2O$) and bilinite ($Fe^{2+}Fe_2^{3+}(SO_4)_4 \cdot 22H_2O$). These techniques have been proven to give valuable insight into the structure of apjohnite and pickeringite (Mn and $Mg^{2+}$ halotrichites respectively) by previous works of the authors [3].

## Material and methods

*Preparation of halotrichite*

Saturated solutions of iron(III) sulphate hydrate ($Fe_2(SO_4)_3 \cdot H_2O$), iron(II) sulphate heptahydrate ($FeSO_4 \cdot 7H_2O$), and aluminium sulphate octadecahydrate ($Al_2(SO_4)_3 \cdot 18H_2O$) were prepared using AR grade materials. For bilinite, the saturated solution contained $FeSO_4 \cdot 7H_2O$ and $Fe_2(SO_4)_3 \cdot H_2O$, while the saturated solution for halotrichite was comprised of $FeSO_4 \cdot 7H_2O$ and $Al_2(SO_4)_3 \cdot 18H_2O$. Each of the substances used to prepare the saturated solution were then placed in the centre of separate Whatman 540 filter papers with a one mole ratio. The filter paper was then tied with cotton to form a bag with the sulphate salt contained inside. The saturated solution was placed in a beaker and a bag of each of the sulphate salts used to prepare the saturated solution was attached on opposite sides of the beaker. The beaker was covered with Parafilm and left for a period of a week to allow for the halotrichite compound to crystallise. Crystals collected from the beaker were then washed with diethyl either and dried overnight in an oven (85 °C).

*X-ray diffraction*

X-ray diffraction patterns were collected using a Philips X'pert wide angle X-ray diffractometer, operating in step scan mode, with Cu Kα radiation (1.54052 Å). Patterns were collected in the range 3 to 90° 2θ with a step size of 0.02° and a rate of 30s per step. Samples were prepared as a finely pressed powder into aluminium sample holders. The Profile Fitting option of the software uses a model that employs twelve intrinsic parameters to describe the profile, the instrumental aberration and wavelength dependent contributions to the profile.

*Mid-IR spectroscopy*

Infrared spectra were obtained using a Nicolet Nexus 870 FTIR spectrometer with a smart endurance single bounce diamond ATR cell. Spectra over the 4000–525 $cm^{-1}$ range were obtained by the co-addition of 64 scans with a resolution of 4 $cm^{-1}$ and a mirror velocity of 0.6329 cm/s. Spectra were co-added to improve the signal to noise ratio.

*Near-infrared (NIR) spectroscopy*

NIR spectra were collected on a Nicolet Nexus FT-IR spectrometer with a Nicolet Near-IR Fibreport accessory (Madison, Wisconsin). A white light source was used, with a quartz

beam splitter and TEC NIR InGaAs detector. Spectra were obtained from 13 000 to 4000 $cm^{-1}$ (0.77-2.50 μm) by the co-addition of 64 scans at a spectral resolution of 8 $cm^{-1}$. A mirror velocity of 1.266 m $sec^{-1}$ was used. The spectra were transformed using the Kubelka-Munk algorithm to provide spectra for comparison with published absorption spectra.

*Spectral analysis*

Band component analysis was undertaken using the Jandel 'Peakfit' (Erkrath, Germany) software package which enabled the type of fitting function to be selected and allows specific parameters to be fixed or varied accordingly. Band fitting was done using a Lorentz-Gauss cross-product function with the minimum number of component bands used for the fitting process. The Lorentz-Gauss ratio was maintained at values greater than 0.7 and fitting was undertaken until reproducible results were obtained with squared correlations ( $r^2$) greater than 0.995. Band fitting of the spectra is quite reliable providing there is some band separation or changes in the spectral profile.

## Results and discussion

*X-ray diffraction*

X-ray diffraction patterns for bilinite, halotrichite and the iron salts used to synthesise the iron halotrichites are given in Figure 1. The synthetic halotrichite XRD pattern matches well with the reference halotrichite pattern 00-039-1387, confirming the successful synthesis of halotrichite. The absence of iron (II) sulphate and aluminium sulphate peaks in the halotrichite sample confirms that a relatively pure halotrichite forms. However, it appears that peaks similar to those observed for bilinite are present in the XRD pattern. This indicates that the oxidation of $Fe^{2+}$ occurs during the synthesis of halotrichite. No reference pattern exists for bilinite so verification of its formation cannot be made directly, however the absence of peaks associated with the iron sulphates salts used in the synthesis procedure suggest that bilinite has been successfully formed. The bilinite structure is significantly more crystalline than the halotrichite sample.

*Mid-infrared spectroscopy*

The infrared spectra have been divided into sections according to the attribution of bands in this spectral region. Accordingly spectra are divided into the spectral region between a) 3800 and 2000 $cm^{-1}$ (Figure 2) and b) 1300 and 700 $cm^{-1}$ (Figure 3). The first spectral region is associated with the OH stretching vibrations whilst the second region is due to $\nu_1$ and $\nu_3$ sulphate antisymmetric stretching modes (~1100 $cm^{-1}$) and weak water librational modes (~900 $cm^{-1}$). The observation of multiple bands infers that non equivalent sulphate anions exist in the structure.

OH stretching region 3800-2500 $cm^{-1}$

The infrared spectrum of halotrichite is extremely complex in the OH stretching region, consisting of eight overlapping bands and ranging from 3600 to 2300 $cm^{-1}$. The spectrum of halotrichite shares a number of similar bands to the starting material aluminium sulphate, however the intensity of bands varies. XRD confirmed that halotrichite formed (with minimal to no aluminium sulphate remaining in the sample). Both halotrichite and aluminium sulphate consist of eight overlapping bands, where halotrichite has bands at 3568, 3494, 3438, 3268, 3002, 2813, 2491, and 2294 $cm^{-1}$ whilst aluminium sulphate has bands at 3610, 3516, 3427, 3256, 3004, 2824, 2458, and 2293 $cm^{-1}$. This suggests that the halotrichite sample shares a number of similar OH stretching environments as aluminium sulphate. The spectrum of halotrichite shows a shift to lower wavenumbers, especially for bands observed between 3600 and 3400 $cm^{-1}$. This shift is due to a reduction in the number of OH stretching vibrations associated with Al-OH due to the introduction of Fe-OH stretching vibrations. The shape of the band profile for halotrichite in the higher wavenumber region resembles that of bilinite and iron (III) sulphate. This suggests two things 1) both Fe-OH and Al-OH vibrations exist and 2) oxidation of the $Fe^{2+}$ ion occurred during the synthesis of halotrichite resulting in a small portion of $Fe^{3+}$ to be incorporated into the structure. Comparison of the XRD patterns of halotrichite and bilinite show common peaks at 9 and 14° 2θ also indicating the oxidation of $Fe^{2+}$. However, the formation of halotrichite is predominant. The overall band profile differs between aluminium sulphate and halotrichite, shown by a significant increase in the intensity of the band at around 3250 $cm^{-1}$. This increase in intensity is due to the Fe-OH stretching vibrations. Combining the spectra of aluminium sulphate and iron (II) sulphate shows that a shoulder at around 3300 $cm^{-1}$ would result in the aluminium sulphate spectrum as seen for halotrichite.

The spectrum of bilinite resembles the spectrum of iron(III) sulphate largely. Bilinite ($Fe^{2+}Fe_2^{3+}(SO_4)\cdot 22H_2O$) has a higher quantity of $Fe^{3+}$ in its structure and therefore similarities between iron (III) sulphate are expected. However, differences in the two spectra confirm that a new structure has formed. The overall band profile of bilinite and halotrichite differ significantly, shown by the absence of an intense broad band at around 3000 $cm^{-1}$ observed for both halotrichite and aluminium sulphate. This indicates that the band at 3000 $cm^{-1}$ is associated with aluminium in the halotrichite structure. The higher wavenumber region of bilinite is similar to iron (III) sulphate, and therefore the small sharper bands at high wavenumbers are due to the iron-OH stretching vibrations of $Fe^{3+}$ and $Fe^{2+}$. Bands assigned to $Fe^{2+}$ (~3530 $cm^{-1}$) are at lower wavenumbers compared to the $Fe^{3+}$ (~3570 $cm^{-1}$) bands. The width of the overall band profile for bilinite is a lot more condensed than halotrichite. Halotrichite observed bands at 2491 and 2294 $cm^{-1}$, while these bands are absent for bilinite.

$SO_4^{2-}$ stretching region 1200-800 $cm^{-1}$

The spectra of bilinite and halotrichite are highly complex in this spectral region with up to 12 overlapping bands, Figure 3. This indicates that both halotrichite samples have multiple sulphate anions in slightly different environments. The $\nu_1$ symmetric stretching sulphate bonds are observed between 1000 and 900 $cm^{-1}$, and it can be clearly observed in Figure 3 that significant differences in the intensities of these bands exist for bilinite and halotrichite. The sharpest band for bilinite, observed at 985 $cm^{-1}$ is proposed to be due to sulphate anions associated with $Fe^{3+}$. A similar band is observed for iron (III) sulphate. The most intense band observed for halotrichite is observed at higher wavenumbers, between 1070 and 1050 $cm^{-1}$. These bands are assigned to the $\nu_3$ stretching modes of sulphate. The positions of the bands correspond well with bands observed for the iron (II) sulphate spectrum, and therefore it is proposed that these sulphate bands are associated with the $Fe^{2+}$ ions. The presence of bands at lower wavenumbers for halotrichite (990 to 900 $cm^{-1}$) again reinforces the slight formation of bilinite during the synthesis of halotrichite. However, as it has been shown by different techniques and spectral regions discussed, halotrichite is the predominate phase that forms. Higher wavenumber bands (1200 to 1100 $cm^{-1}$) are observed for both bilinite and halotrichite and are assigned to
$\nu_3$ ($SO_4^{2-}$).

*Near-infrared (NIR) spectroscopy*

199

200 Electronic bands of transition metals 12500-7500 $cm^{-1}$

201

202 This spectral region includes electronic bands resulting from transition metal ions in the
203 structure and also bands related to the second fundamental overtones of the OH stretching
204 vibrations [4-11]. The NIR spectra of halotrichite and bilinite in this spectral region are
205 provided in Figure 4. No bands exist in this range for aluminium sulphate and therefore have
206 been excluded from Figure 4. There are two features in this spectral region that are
207 noteworthy and they are the broad bands centred around 8550 and 10900$cm^{-1}$. These bands
208 are attributed to electronic bands of the ferrous ion [12-14]. Comparison of the spectra of
209 bilinite and halotrichite shows that $Fe^{2+}$ used in the synthesis of halotrichite oxidises to $Fe^{3+}$
210 shown by the broadness of the band centred at around 10900 $cm^{-1}$. If pure halotrichite had
211 formed a less broad band centred at 11200 $cm^{-1}$ would have been observed similar to iron (II)
212 sulphate. It is also observed that the ratio of the intensities of the bands at 11200 and 8500
213 $cm^{-1}$ for iron (II) sulphate are reversed for halotrichite. This observation again reinforces the
214 fact that the oxidation of $Fe^{2+}$ has occurred during the synthesis procedure, and therefore
215 bilinite has crystallised along with halotrichite. The IR spectra and XRD patterns have shown
216 that halotrichite is the primary mineralogical phase that formed. To minimise the formation of
217 bilinite preventative measures (such as a nitrogen atmosphere) need to be incorporated into
218 the synthesis of halotrichite. The presence of the band centred at 8400 $cm^{-1}$ for bilinite
219 confirms that both $Fe^{2+}$ and $Fe^{3+}$ are present in the structure, which provides further evidence
220 that bilinite has indeed formed.

221

222 Water OH overtones and sulphate combination bands 5400-4400 $cm^{-1}$

223

224 The spectral region between 5400 and 4400 $cm^{-1}$ is ascribed to the water OH overtones and
225 sulphate combination bands, Figure 5. There are minimal differences between bilinite and
226 halotrichite in this spectral region, suggesting that the influence of iron and aluminium are
227 minimal. Therefore, these bands are believed to be due to water and sulphate bands in the
228 halotrichite samples. Based on the fact that both bilinite and halotrichite essentially have the
229 same overall spectral profile in this region it is proposed that water and sulphate are in similar
230 environments for both samples. This confirms that a halotrichite structure forms for bilinite.
231 Slight shifts in wavenumbers between halotrichite and bilinite are due to the substitution of
232 $Al^{3+}$ for $Fe^{3+}$, respectively. An additional band at 4510 $cm^{-1}$ is observed for halotrichite and is

also observed for iron (II) sulphate. This reinforces that not all $Fe^{2+}$ oxidised to $Fe^{3+}$ in the synthesis of halotrichite.

## Conclusions

This investigation has shown that halotrichite and bilinite were successfully synthesised and characterised by infrared and near-infrared spectroscopy. Synthesis of the two synthetic halotrichites has shown the effect of $Al^{3+}$ for $Fe^{3+}$ in the halotrichite structure. Changes in the overall band profile for the two synthetic halotrichites has then allowed for bands associated with $Fe^{2+}$ and $Fe^{3+}$ to be identified and thus used in the verification of the formation of bilinite. Similar band profiles indicate that bilinite shares a similar structure to that as halotrichite, and therefore is proposed to have been successfully synthesised. XRD and NIR have shown that halotrichite has a slight contamination of bilinite due to the oxidation of $Fe^{2+}$ to $Fe^{3+}$ during the synthesis process.

## Acknowledgments

The financial and infra-structure support of the Queensland University of Technology, Inorganic Materials Research Program is gratefully acknowledged. The Australian Research Council (ARC) is thanked for funding the instrumentation.

## References


[1] S. Menchetti, C. Sabelli, Min. Mag.. 40 (1976) 599-608.

[2] S.D. Ross, Inorganic Infrared and Raman Spectra, Mineralogical Society, London, 1974.

[3] S. Palmer, R.L. Frost, Polyhedron 25 (2006) 3379-3386.

[4] R.L. Frost, S.J. Palmer, B.J. Reddy, Vib. Spectrosc. 44 (2007) 154-161.

[5] R.L. Frost, B.J. Reddy, D.L. Wain, W.N. Martens, Spectrochim. Acta 66A (2007) 1068-1074.

[6] S. Palmer, B.J. Reddy, R.L. Frost, Polyhedron 26 (2007) 524-533.

[7] B.J. Reddy, L. Frost Ray, Spectrochim. Acta 66A (2007) 312-317.

[8] B.J. Reddy, R.L. Frost, J. Near Infrared Spectrosc. 15 (2007) 115-121.

[9] B.J. Reddy, L. Frost Ray, W.N. Martens, D.L. Wain, J.T. Kloprogge, Vib. Spectrosc. 14 (2007) 42-49.

[10] B.J. Reddy, L. Frost Ray, M.L. Weier, W.N. Martens, J. Near Infrared Spectrosc. 14 (2006) 241-250.

[11] R. L. Frost R.A. Wills, W.N. Martens, M.L. Weier, B.J. Reddy, Spectrochim. Acta 62A (2005) 42-50.

[12] G.R. Rossman, M.N. Taran, Am. Mineral.. 86 (2001) 199-210.

[13] M.N. Taran, K. Langer, Chem. Miner. 28 (2001) 199-210.

[14] M.N. Taran, G.R. Rossman, Am. Mineral. 86 (2001) 973-980.

## List of Figures

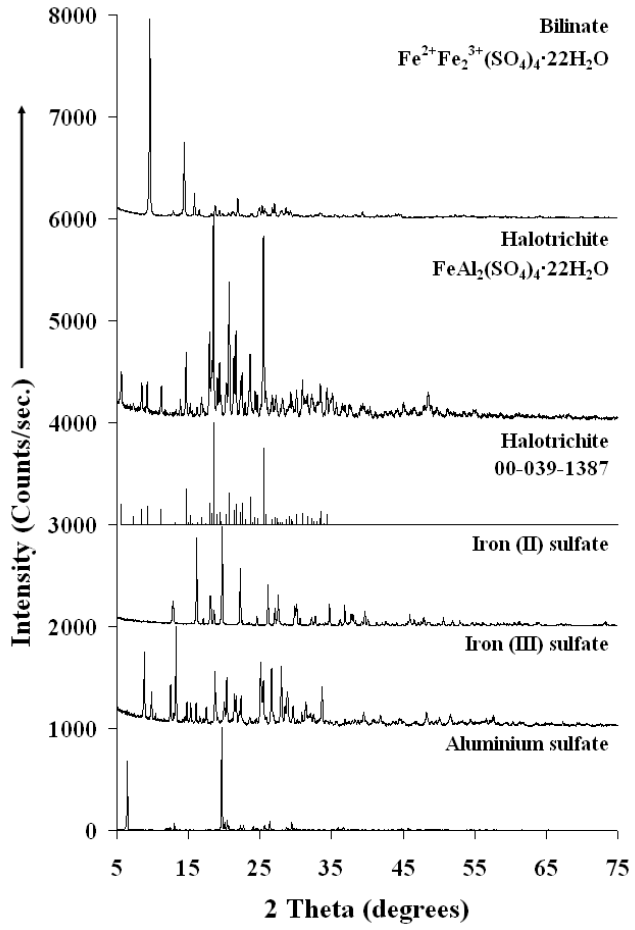


304

305 **Figure 1**

306

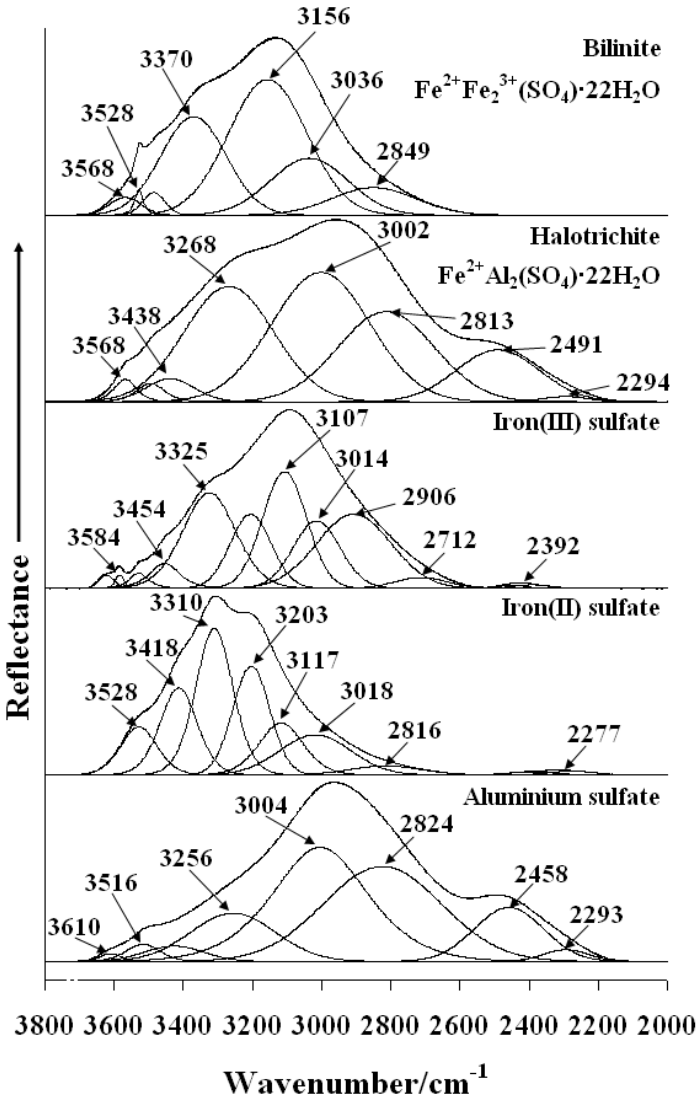


307

308 **Figure 2**

309

310

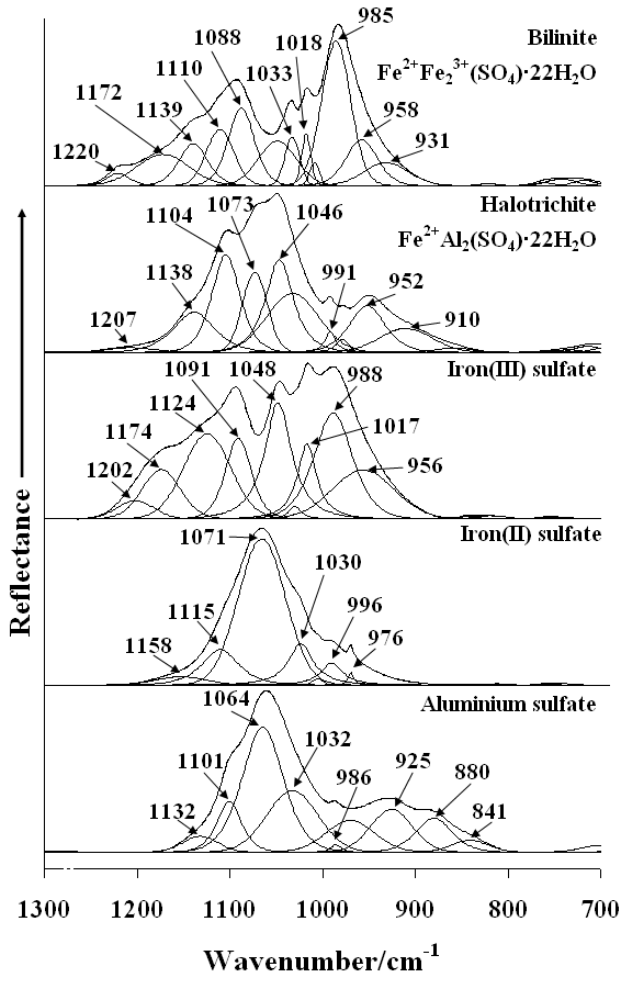


311

312 **Figure 3**

313

314

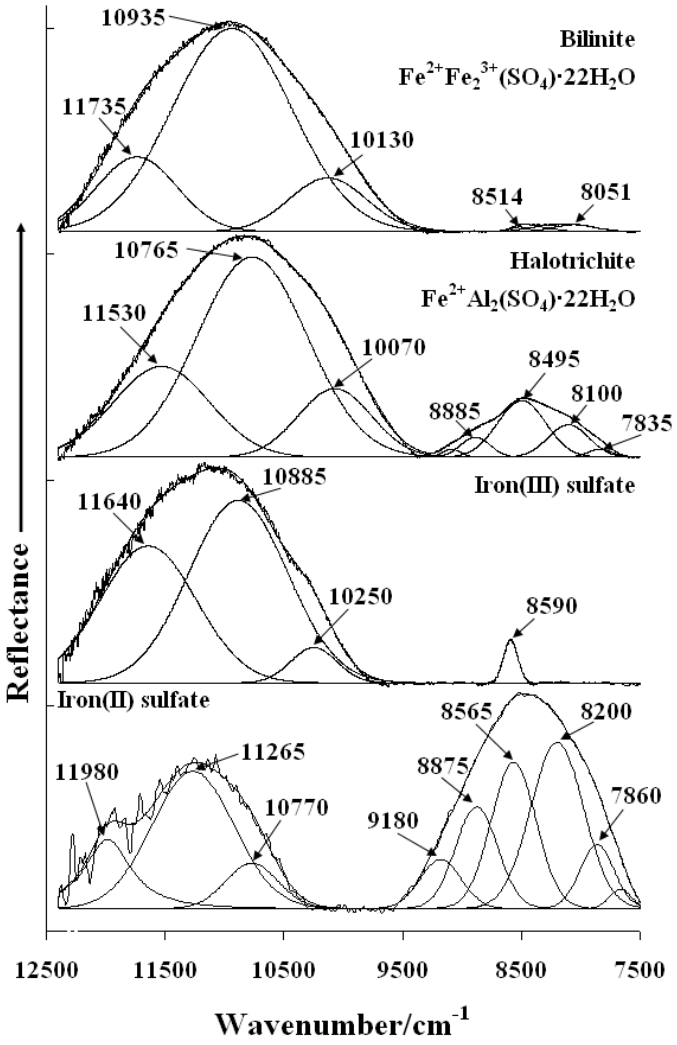


315

316 **Figure 4**

317

318

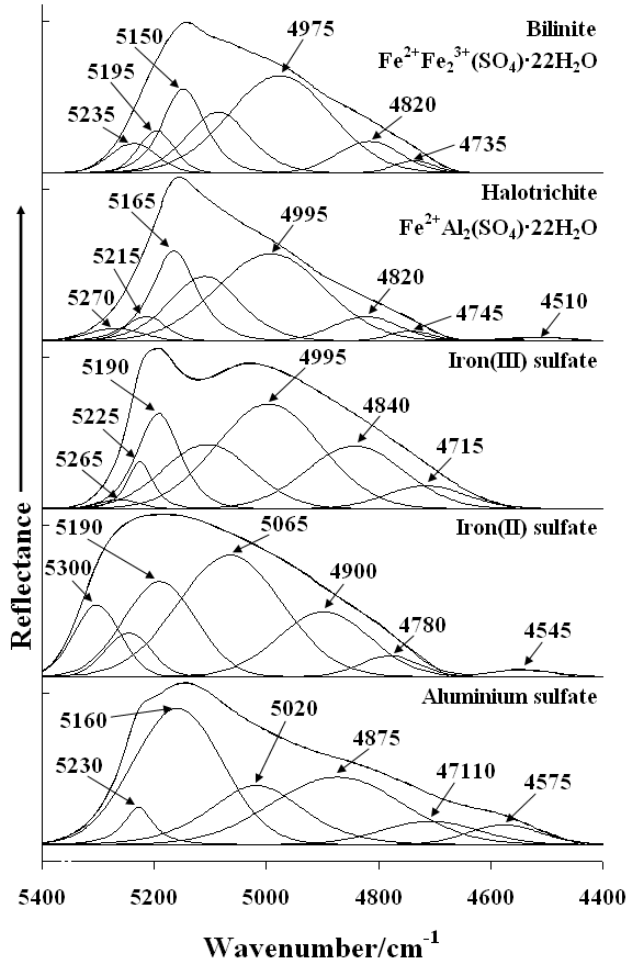


319

320 **Figure 5**

321

322

323